Progressive evolution of silicon surface microstructures via femtosecond laser irradiation in ambient air

Yuncan Ma [a], Jinhai Si [b,*], Xuehui Sun [b], Tao Chen [b], Xun Hou [b]

[a] National Key Laboratory of Shock Wave and Detonation Physics, Institute of Fluid Physics (IFP), China Academy of Engineering Physics (CAEP), No. 64, Mianshan Road, Mianyang, 621900, Sichuan, China
[b] School of Electronics & Information Engineering, Key Laboratory for Physical Electronics and Devices of the Ministry of Education, Collaborative Innovation Center of Suzhou Nano Science and Technology, Xi'an Jiaotong University (XJTU), No. 28, Xianning West Road, Xi'an, 710049, Shaanxi, China

ARTICLE INFO

ABSTRACT

Using 800-nm femtosecond laser irradiation, progressive evolution of the silicon surface microstructures has been demonstrated. Via the variation of laser irradiation parameters, four kinds of microstructures, such as: well-defined and clean nano-ripples, obscured nano-ripples with nano-protrusions and nano-holes, micro-spikes with nano-holes, and separated micro-spikes, have been produced. The morphology and chemical compositions of these microstructures have been characterized by a scanning electronic microscopy equipped with an energy dispersive x-ray spectroscopy. The formation and evolution mechanism of these microstructures have been systematically discussed. Meanwhile, the incorporation mechanism of foreign oxygen species into silicon materials has also been discussed on the basis of the femtosecond laser induced trapping effect of the dangling bonds.

© 2014 Elsevier B.V. All rights reserved.

1. Introduction

Crystalline silicon (*c-Si*) material, which is of great importance in the field of semiconductor industry, has a great amount of applications in silicon devices, such as: photovoltaic cells [1–3], optoelectronic detectors [4,5], micro-electromechanical systems [6,7] and so on. Meanwhile, femtosecond laser microfabrication, which has proved to be an effective technology for producing various micro/nano structures on/in different kinds of materials [8–10], has attracted considerable research attentions.

Recently, femtosecond laser microfabrication has been widely applied to microstructure silicon material under different environments and laser irradiation parameters [11–13], and various kinds of surface micro/nano structures, such as: periodical nano-ripples [14–16], micro-spikes [17–19], micro-grooves [20–22], micro-craters [13] and so on, have been produced. Due to the improvement of the electrical, optical and wetting properties, these microstructures could find some potential and practical applications in silicon photovoltaic cells [23–25], superhydrophobic

surfaces [26,27], and so on. However, in the present reports, most of the silicon surface microstructures were fabricated via single or multiple pulses irradiation on fixed position of the substrates [28–31]. This makes the area of the fabricated microstructures be restricted to a small scale of a laser spot size, which would limit the applications of these microstructures. Meanwhile, as an effective mean for the fabrication of large area (A) microstructures, line by line scanning was usually adopted, however, there have been few reports on the progressive evolution of silicon surface microstructures produced by this mean. Based on this, we predict that the progressive evolution of silicon microstructures via the meaning of line by line scanning would provide useful reference for the fabrication of microstructures with large area. Moreover, the chemical composition of silicon microstructures is of great importance for the applications, incorporation of foreign species would influence the integration property of silicon wafers to other devices, but there have been few reports on this topic. Therefore, the chemical compositions of the silicon microstructures need to be confirmed.

In this paper, the progressive evolution of femtosecond laser induced silicon surface microstructures with large area, which was achieved by the mean of line by line scanning, was demonstrated. The morphology and chemical compositions of these structures were characterized by a scanning electronic microscopy (SEM) equipped with an energy dispersive x-ray spectroscopy (EDX),

* Corresponding author. Tel.: +86 15182490746.
E-mail addresses: jinhaisi@mail.xjtu.edu.cn, mayuncan2014@gmail.com, 59365722@qq.com, mayuncan2013@163.com, jinhaisi@mail.xjtu.edu.cn (J. Si).
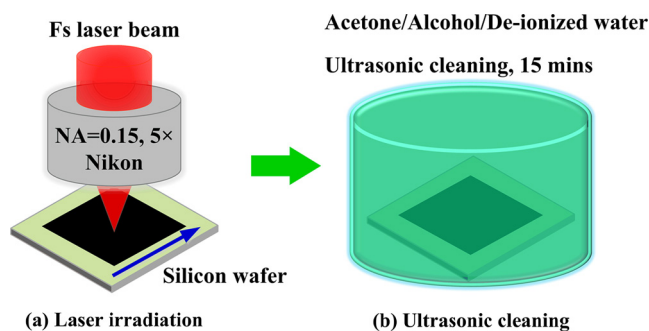
Fig. 1. (Color online) Technological process for fabrication of silicon surface microstructures. (a) Laser irradiation; (b) Ultrasonic cleaning.

respectively. By controlling the laser energy accumulated on the silicon substrates, four classical kinds of surface microstructures, which could be called as: well-defined and clean nano-ripples, obscured nano-ripples with nano-protrusions and nano-holes, micro-spikes with nano-holes, and separate micro-spikes, were produced. The formation and evolution mechanism of these structures were systematically discussed. Furthermore, according to the results from EDX measurement, foreign oxygen species was incorporated into silicon material, and the incorporation mechanism of foreign oxygen species was discussed on the basis of the femtosecond laser induced trapping effect of dangling bonds.

2. Experimental details

The technological process for the fabrication of silicon surface microstructures could be divided chronologically to two steps, which have been illustrated in Fig. 1.

2.1. Laser irradiation

Prior to the femtosecond laser irradiation, in order to eliminate the influence of the surrounding or covering contaminations on the laser irradiation, the single polished p-type silicon wafers, with the orientation of (1 0 0), the thickness of 300 μm, were rinsed in an ultrasonic cleaner with acetone, ethanol, and de-ionized water for 10 min, respectively.

Then these clean silicon wafers were mounted horizontally onto a computer controlled three dimensional (3D) translation stage (Pro Scan II™) with a step resolution of 40 nm at x, y, z directions, respectively. An amplified Ti: sapphire femtosecond laser system (Coherent Inc., U.S.A.), which delivered laser pulses with 50-fs pulse duration, 800-nm central wavelength, and 1-kHz repetition rate, was employed as the light source in our experiments. The intensity distribution of laser beam was Gaussian-type. The laser average power (P) could be continuously varied by rotating a variable neutral density filter (NDF), and the access of the laser beam was controlled via a mechanical shutter connected to the computer. The horizontally polarized femtosecond laser beam was focused perpendicularly onto silicon wafers by a microscope objective lens (NA = 0.15, 5×, Nikon), the size of the laser spot (D = 30 μm) was determined by measuring the diameter of the photoinduced craters via a single laser pulse irradiation on the substrate, and then the laser average fluence (F) was calculated by the formula $F = \frac{P}{f \cdot \pi \cdot (D/2)^2}$, here f is the repetition rate of the incident laser. The laser scanning direction, which has been illustrated as blue arrow line in Fig. 1(a), was parallel to the polarization direction of the incident laser. The laser scanning velocity (υ), the scanning length (L), the distance between two adjacent scanning lines (Δd) and the number of scanning lines (N) could be set via the software equipped with the 3D translation stage. A charge coupled device (CCD) camera, which was connected with the computer, was used to monitor the laser irradiation process online. Meanwhile, the whole femtosecond laser irradiation process was conducted in ambient air, with the temperature and humidity of 25 °C and 45%, respectively.

2.2. Ultrasonic cleaning

After femtosecond laser irradiation, all the silicon wafers were rinsed in an ultrasonic cleaner with acetone, ethanol, and de-ionized water for 15 min, respectively. During ultrasonic shocking process, the temperature of surrounding liquid raised from 25 °C to 40 °C, and the laser ablation induced debris escaped from silicon surface to surrounding liquids. This would be beneficial to reduce or avoid the influences of the laser ablation induced debris on the morphology and chemical composition of the microstructures.

2.3. Characterization of microstructures

After ultrasonic cleaning, all the irradiated silicon wafers were placed in a fume hood for 30 min until they were dry. Then the morphology and chemical compositions of the silicon-based surface microstructures were characterized by a scanning electronic microscopy (SEM, FEI Quanta 250 FEG Serials) equipped with an energy dispersive X-ray spectroscopy (EDS, TEAM™ Serials), respectively.

3. Results and discussion

3.1. Microstructure evolution under different laser average fluences

Fig. 2 illustrates the progressive evolution of the femtosecond laser induced silicon surface microstructures under different laser average fluences (F). The laser irradiation parameters were: NA = 0.15, 5×, υ = 800 μm s^{-1}, L = 1.5 cm, Δd = 10 μm, A = 1.5 cm × 1.5 cm, N = 1500, F = 0.21 J cm^{-2}, 0.35 J cm^{-2}, 0.48 J cm^{-2}, 0.63 J cm^{-2}, 0.76 J cm^{-2}, 0.90 J cm^{-2}.

It can be seen from Fig. 2 that the silicon surface microstructures undergo successive evolutions with the increase of laser average fluence. Four kinds of structures, which could be called as: well-defined and clean nano-ripples (Fig. 2(a)), obscured nano-ripples with nano-protrusions and nano-holes (Fig. 2(b) and Fig. 2(c)), micro-spikes surrounding with nano-holes (Fig. 2(d)), and separate micro-spikes (Fig. 2(e) and Fig. 2(f)), have been produced on silicon surface.

When the laser average fluence was 0.21 J cm^{-2}, which was close to the ablation threshold of the silicon material, well-defined and clean nano-ripples were produced. It can be seen from Fig. 2(a) that these nano-ripples, with the orientation perpendicular to the direction of the incident laser polarization, have a period (Λ) of about 600–700 nm. This is in well accordance with the present literatures [32–35]. As for the formation mechanism of these nano-ripples, the interference between the incident laser and the laser induced surface plasmons is reasonable. When the femtosecond laser with high intensity irradiated onto the silicon substrates, there would be plenty of surface plasmas came into being, and the surface plasma wave would interfere with the incident femtosecond laser, then the laser energy accumulated on the silicon surface would be periodically modulated. This would result in periodically modulated ablation to silicon surface. Therefore, the periodical nano-ripples formed.

When the laser average fluence was 0.35 J cm^{-2}–0.48 J cm^{-2}, which was slightly higher than the ablation threshold of silicon material, obscured nano-ripples were produced. It can be seen from Fig. 2(b) and (c) that these nano-ripples were covered or
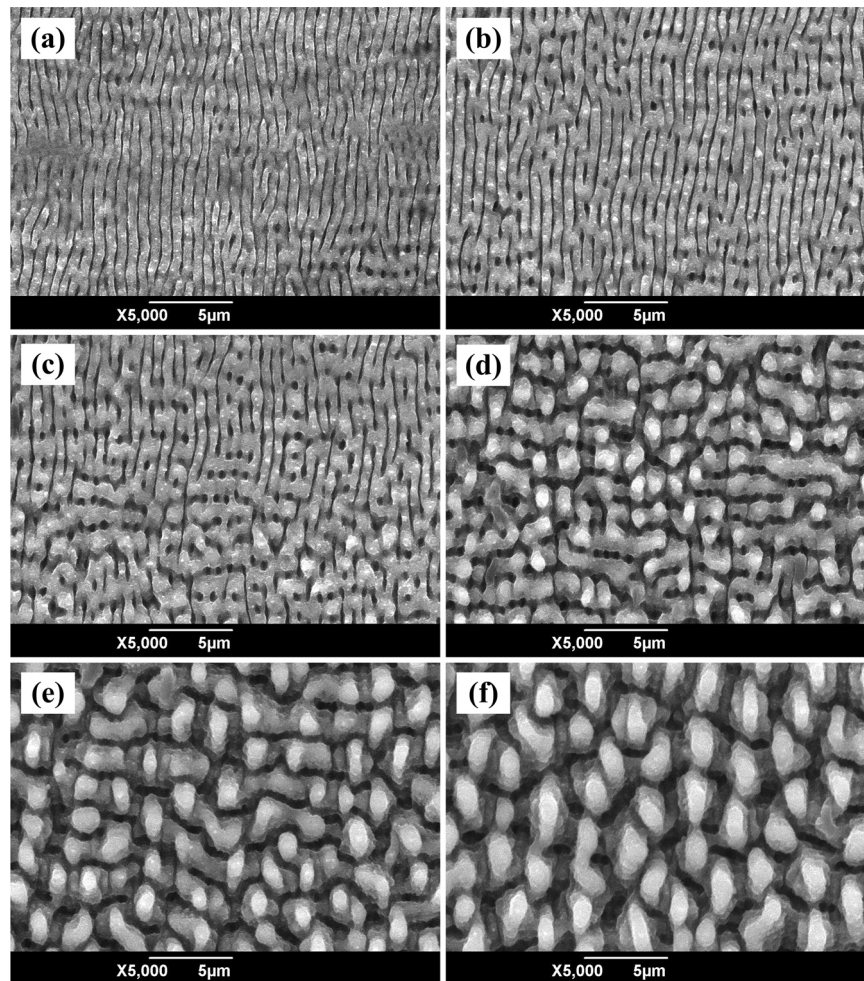
Fig. 2. Progressive evolution of silicon surface microstructures under different laser average fluences. (a) 0.21 J cm^{-2}; (b) 0.35 J cm^{-2}; (c) 0.48 J cm^{-2}; (d) 0.63 J cm^{-2}; (e) 0.76 J cm^{-2}; (f) 0.90 J cm^{-2}.

surrounded by some nano-protrusions and nano-holes, and this makes the nano-ripples look obscured. The formation mechanism of these obscured nano-ripples could also be explained by the modulation ablation of the incident femtosecond laser pulses. Since the laser average fluence was slightly higher that the ablation threshold of silicon material, original well-defined and clean nano-ripples would be induced during the first few preceding laser pulses irradiation, subsequent laser energy accumulated on the silicon surface would be modulated by the coarse silicon surface covered with these obscured nano-ripples. More exactly speaking, the incident laser fluence accumulated on the silicon substrate was non-uniform. This would make some melt silicon materials be formed on the nano-ripples, and these melt silicon materials were not stable, they would flow under the interaction of the surface tension. Then some nano-protrusions with the scale of 600 nm–700 nm formed on the ripples, and several random nano-holes with the scale of 200 nm–300 nm formed between two adjacent nano-ripples.

When the laser average fluence was 0.63 J cm^{-2}, which was much higher than the ablation threshold of silicon material, micro-spikes with the scale of about 1 μm were produced. It can be seen from Fig. 2(d) that these micro-spikes were surrounding with some nano-holes, and the nano-ripples as those shown in Fig. 2(b) and (c) disappeared. The formation mechanism of these micro-spikes could be well explained with the schematic illustration in Fig. 3. Since the laser fluence was much higher than the ablation threshold of silicon material, the first few preceding laser pulses irradiation
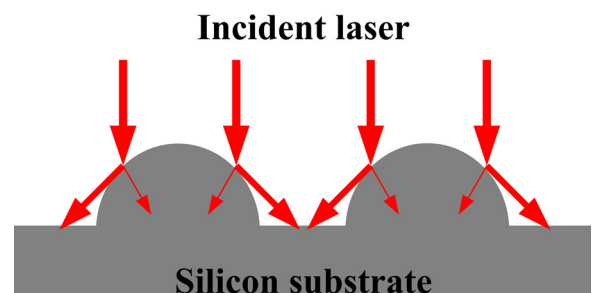

Fig. 3. (Color online) Schematic illustration for the formation mechanism of micro-spikes on silicon surface.

would make the nano-ripples with nano-protrusions and nano-holes be produced. The existence of these nano-protrusions and nano-holes were beneficial to the subsequent laser pulses being coupled deeper into the silicon material. It can be seen from Fig. 3 that the incident laser pulses were reflected by these pro-trusions. The smaller the corner angle of the micro-spikes, the more and the deeper the laser energy coupled into the silicon material.

When the incident laser average fluence was 0.76 J cm^{-2}–0.90 J cm^{-2}, separate micro-spikes were produced, as shown in Fig. 2(e) and (f). The formation mechanism of the separated micro-spikes has been stated on the related references. Under the irradiation of higher laser average fluence, more and
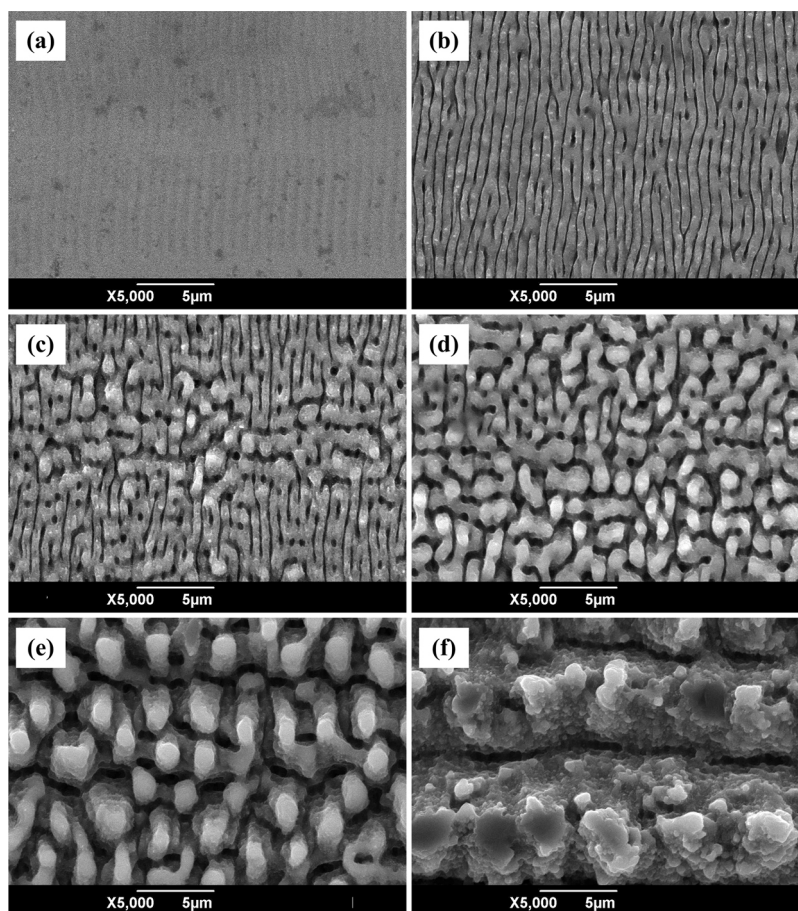
Fig. 4. Progressive evolution of silicon surface microstructures under different laser scanning velocities. (a) 2000 μm s^{-1}; (b) 1600 μm s^{-1} (c) 1200 μm s^{-1}; (d) 800 μm s^{-1}; (e) 400 μm s^{-1}, (f) 100 μm s^{-1}.

more laser energy were coupled onto silicon material. This makes more material between adjacent protrusions transform from solid state to liquid state. That was to say, the silicon material melt. And then the nucleation of the liquid silicon occurred at the gas-solid interface, which resulted in the formation of separate micro-spikes. This effect has been reported as solidification driven extrusion [36–38]. Furthermore, it can be seen from Fig. 2(e) and (f) that the top shape of these micro-spikes was ellipse, and the orientation of the long axis of the ellipse was the same as that of the nano-ripples formed under small laser fluence, which indicated that these micro-spikes grew from the original nano-ripples.

3.2. Microstructure evolution under different laser scanning velocities

Fig. 4 illustrates the progressive evolution of the femtosecond laser induced silicon surface microstructures under different laser scanning velocities (υ). The laser irradiation parameters were: NA = 0.15, 5×, L = 1.5 cm, $\triangle d$ = 10 μm, A = 1.5 cm × 1.5 cm, N = 1500, F = 0.92 J cm^{-2}, υ = 2000 μm s^{-1}, 1600 μm s^{-1}, 1200 μm s^{-1}, 800 μm s^{-1}, 400 μm s^{-1}, 100 μm s^{-1}.

It can be seen from Fig. 4 that the silicon surface microstructures under different laser scanning velocities show the same variations as those under different laser average fluences. When the laser scanning velocity was ranged from 1600 μm s^{-1} to 2000 μm s^{-1}, well-defined and clean nano-ripples with a period of 600 nm–700 nm, as shown in Fig. 4(a) and Fig. 4(b), were produced. When the laser scanning velocity decreased to 1200 μm s^{-1}, obscured nano-ripples with nano-protrusions and nano-holes, as

shown in Fig. 4(c), came into being. When the laser scanning velocity further decreased to 800 μm s^{-1}, micro-spikes with nano-holes, as shown in Fig. 4(d), were fabricated. When the laser scanning velocity was 400 μm s^{-1}, separate micro-spikes, as shown in Fig. 4(e), formed on the silicon surface. This evolution could be well understood by the laser energy accumulated on silicon surface modulated by the laser scanning velocities. Under the same laser average fluence, the larger the laser scanning velocity, the smaller the laser energy accumulated on the silicon surface, therefore, the well-defined and clean nano-ripples were produced at higher laser scanning velocity, while the separate micro-spikes were produced at lower laser scanning velocity. However, the laser scanning velocity should be well controlled within a certain range; otherwise the structures would be dramatically destroyed due to the over-accumulation of the laser energy on silicon surface, as shown in Fig. 4(f).

These silicon microstructures, especially the separate micro-spikes with large area, would find some potential applications in silicon devices due to the improvements of optical and wetting properties. For example, the absorption and luminescence of silicon material would be greatly enhanced thanks to the existence of micro-spikes; therefore, this silicon material has been usually called as "black silicon". This would be beneficial to the fabrication of silicon-based photovoltaic cells [23–25], optoelectronics detectors [39–41] and luminescence devices [42,43]. Meanwhile, the hydrophobicity of the silicon surface with these micro-spikes would be greatly improved due to the contact angle increase to over 150°. This makes "black silicon" a good candidate for super-hydrophobic microstructures.
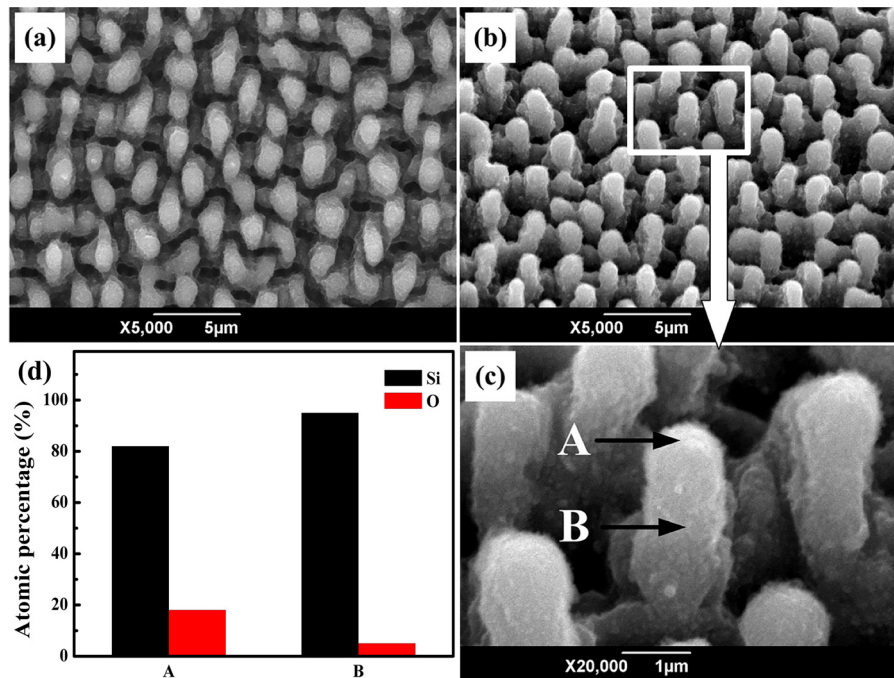
Fig. 5. (Color online) Chemical composition analysis of the silicon micro-spikes. (a) Morphology of the micro-spikes at the silicon surface; (b) Morphology of the micro-spikes at the angle of 45° from the silicon surface; (c) Enlarged morphology of the zone marked in (b); (d) Atomic percentage of silicon and oxygen species.

It should be noted that the evolution of these silicon microstructures with large area were achieved by the mean of line by line scanning. In present reports [28–31], most of the femtosecond laser induced evolution of surface microstructures were accomplished by the mean of single or multiple pulses irradiation on fixed position; this was not beneficial to the fabrication of silicon microstructures with large area. Therefore, the mean of line by line scanning adopted here would provide useful reference for the fabrication of silicon microstructures with large area.

In the above sections, the formation and evolution mechanism of the silicon surface microstructures have been discussed. In the following section, the chemical compositions of the microstructures were analyzed, and the incorporation mechanism of the foreign oxygen (O) species into the interior of silicon material will be discussed.

3.3. Incorporation mechanism of oxygen species into silicon material

Fig. 5 illustrates the chemical compositions of the silicon surface micro-spikes. The laser irradiation parameters were: NA = 0.15, 5×, υ = 800 μm s^{-1}, L = 1.5 cm, Δd = 10 μm, A = 1.5 cm × 1.5 cm, N = 1500, F = 0.90 J cm^{-2}. The parameters of EDX measurement were: accelerating voltage Vac = 2.5 kV, emission current I = 91 mA, working distance D = 21.6 mm, and vacuum pressure P = 5.0 × 10^{-4} Pa.

During the process of chemical compositions analysis, points A and B (marked out in Fig. 5(c)) on the micro-spike were selected as the analysis points. It can be seen from Fig. 5(d) that the main chemical compositions of the femtosecond laser induced micro-spike were silicon and oxygen species. At point A, the atomic percentage of silicon species was 81.72% and that of oxygen species was 18.28%, with the error limit of 8.76% and 4.23% respectively; at point B, the atomic percentage of silicon species was 94.34% and that of oxygen species was 5.66%, with the error limit of 9.42% and 2.39%, respectively. These results from EDX measurements indicated that the foreign oxygen species were incorporated into silicon material during femtosecond laser irradiation in ambient air. As for

the incorporation mechanism of oxygen species into silicon material, we employed the femtosecond laser induced trapping effect of dangling bonds to explain it [43,44]. When the femtosecond laser pulses with high fluence irradiated the silicon materials in ambient air, there would be two kinds of phenomenon appear simultaneously. Firstly, under the irradiation of the incident laser pulses, some defects would be induced in silicon materials, and some silicon materials transformed from crystal silicon (c-Si) to amorphous silicon (a-Si). That was to say, original crystal structure of silicon was destroyed, and the bonds between two adjacent silicon atoms was broken, then the dangling bonds appeared in silicon materials. Secondly, under the irradiation of the incident laser pulses, the oxygen in ambient air was photoionized, and there were much oxygen ions surrounding the silicon materials at the laser irradiation zones. Since the dangling bonds have the capacity of trapping the surrounding oxygen atoms, foreign oxygen species was incorporated into the silicon materials, and these oxygen atoms exist in silicon materials in the form of silicon oxides. As far as we investigated, the incorporated oxygen species in silicon material would influence the integration of silicon-based chips with other devices; therefore, the results demonstrated here indicated that some post-treatments for the silicon microstructures would be necessary for the elimination of foreign oxygen species, and the related works have been reported [45].

4. Conclusions

In conclusions, the progressive evolution of femtosecond laser induced silicon surface microstructures, such as: well-defined and clean nano-ripples, obscured nano-ripples with nano-protrusions and nano-holes, micro-spikes with nano-holes, and separated micro-spikes, have been demonstrated under different laser average fluences and laser scanning velocities, respectively. The formation and evolution mechanism of these microstructures was assigned to the modulated laser ablation. Moreover, the chemical compositions of the silicon surface micro-spikes have been analyzed, and the incorporation mechanism of foreign oxygen

species into silicon material was attributed to the femtosecond laser induced trapping effect of the dangling bonds.

References

[1] M. Liu, M.B. Johnston, H.J. Snaith, Efficient planar heterojunction perovskite solar cells by vapour deposition, Nature 501 (2013) 395–398.
[2] N.D. Bronstein, L. Li, L. Xu, Y. Yao, V.E. Ferry, A.P. Alivisatos, R.G. Nuzzo, Luminescent solar concentration with semiconductor nanorods and transfer-printed micro-silicon solar cells, ACS Nano 8 (2014) 44–53.
[3] C. Battaglia, X. Yin, M. Zheng, I.D. Sharp, T. Chen, S. McDonnell, A. Azcatl, C. Carraro, B. Ma, R. Maboudian, R.M. Wallace, A. Javey, Hole selective MoOx contact for silicon solar cells, Nano Lett. 14 (2014) 967–971.
[4] I. Goykhman, B. Desiatov, J. Khurgin, J. Shappir, U. Levy, Locally oxidized silicon surface-plasmon Schottky detector for telecom regime, Nano Lett. 11 (2011) 2219–2224.
[5] D. Marris-Morini, L. Virot, C. Baudot, J.M. Fedeli, G. Rasigade, D. Perez-Galacho, J.M. Hartmann, S. Olivier, P. Brindel, P. Crozat, F. Boeuf, L. Vivien, A 40 Gbit/s optical link on a 300-mm silicon platform, Opt. Express 22 (2014) 6674–6679.
[6] K. Yamamoto, F. Goericke, A. Guedes, G. Jaramillo, T. Hada, A.P. Pisano, D. Horsley, Pyroelectric aluminum nitride micro-electromechanical systems infrared sensor with wavelength selective infrared absorber, Appl. Phys. Lett. 104 (2014) 111111.
[7] J. Suh, A.J. Weinstein, K.C. Schwab, Optomechanical effects of two-level systems in a back-action evading measurement of micro-mechanical motion, Appl. Phys. Lett. 103 (2013) 052604.
[8] R.R. Gattass, E. Mazur, Femtosecond laser micromachining in transparent materials, Nature Photonics 2 (2008) 219–225.
[9] Y. Cheng, K. Sugioka, K. Midorikawa, M. Masuda, K. Toyoda, M. Kawachi, K. Shihoyama, Control of the cross-sectional shape of a hollow microchannel embedded in photostructurable glass by use of a femtosecond laser, Opt. Lett. 28 (2003) 55–57.
[10] C. Li, X. Shi, J. Si, T. Chen, F. Chen, S. Liang, Z. Wu, X. Hou, Alcohol-assisted photoetching of silicon carbide with a femtosecond laser, Opt. Commun. 282 (2009) 78–80.
[11] M. Shen, J.E. Carey, C.H. Crouch, M. Kandyla, H.A. Stone, E. Mazur, High-density regular arrays of nanometer-scale rods formed on silicon surfaces via femtosecond laser irradiation in water, Nano Lett. 8 (2008) 2087–2091.
[12] M.A. Sheehy, L. Winston, J.E. Carey, C.M. Friend, E. Mazur, Role of the background gas in the morphology and optical properties of laser-microstructured silicon, Chem. Mater. 17 (2005) 3582–3586.
[13] H. Liu, F. Chen, X. Wang, Q. Yang, H. Bian, J. Si, X. Hou, Influence of liquid environments on femtosecond laser ablation of silicon, Thin Solid Films 518 (2010) 5188–5194.
[14] B. Tan, K. Venkatakrishnan, A femtosecond laser induced periodical surface structure on crystalline silicon, J. Micromech. Microeng. 16 (2006) 1080–1085.
[15] R.L. Harzic, D. Dorr, D. Sauer, M. Neumeier, M. Epple, H. Zimmermann, F. Stracke, Large-area, uniform, high spatial frequency ripples generated on silicon using a nano-joule femtosecond laser at high repetition rate, Opt. Lett. 36 (2011) 229–231.
[16] G. Miyaji, K. Miyazaki, Role of multiple shots of femtosecond laser pulses in periodic surface nano-ablation, Appl. Phys. Lett. 103 (2013) 071910.
[17] M.Y. Shen, C.H. Crouch, J.E. Carey, R. Younkin, E. Mazur, M. Sheehy, C.M. Friend, Formation of regular arrays of silicon micro-spikes by femtosecond laser irradiation through a mask, Appl. Phys. Lett. 82 (2003) 1715–1717.
[18] S. Liu, J. Zhu, Y. Liu, L. Zhao, Laser induced plasma in the formation of surface-microstructured silicon, Mater. Lett. 62 (2008) 3881–3883.
[19] Y. Peng, M. Hong, Y. Zhou, D. Fang, X. Chen, B. Cai, Y. Zhu, Influence of femtosecond laser pulse number on spike geometry of microstructured silicon, Appl. Phys. Exp. 6 (2013) 051303.
[20] T.H.R. Crawford, A. Borowiec, H.K. Haugen, Femtosecond laser micromachining of grooves in silicon with 800 nm pulses, Appl. Phys. A 80 (2005) 1717–1724.
[21] Y. Ma, H. Shi, J. Si, H. Ren, T. Chen, X. Hou, High-aspect-ratio grooves fabricated in silicon by a single pass of femtosecond laser pulses, J. Appl. Phys. 111 (2012) 093102.
[22] Y. Ma, A. Pan, J. Si, T. Chen, F. Chen, X. Hou, A simple method for fabrication of high-aspect-ratio all-silicon grooves, Appl. Surf. Sci. 284 (2013) 372–378.
[23] V.V. Iyengar, B.K. Nayak, M.C. Gupta, Optical properties of silicon light trapping structures for photovoltaics, Sol. Energ. Mater. Sol. C. 94 (2010) 2251–2257.
[24] M.J. Sher, M.T. Winkler, E. Mazur, Pulsed-laser hyperdoping and surface texturing for photovoltaics, MRS Bull. 36 (2011) 439–445.
[25] B.K. Nayak, V.V. Iyengar, M.C. Gupta, Efficient light trapping in silicon solar cells by ultrafast-laser-induced self-assembled micro/nano structures, Prog. Photovoltaics: Res. Appl. 19 (2011) 631–639.
[26] T. Baldacchini, J.E. Carey, M. Zhou, E. Mazur, Superhydrophobic surfaces prepared by microstructuring of silicon using a femtosecond laser, Langmuir 22 (2006) 4917–4919.
[27] A.Y. Vorobyev, C. Guo, Laser turns silicon superwicking, Opt. Express 18 (2010) 6455–6460.
[28] B.R. Tull, J.E. Carey, E. Mazur, J.P. McDonald, S.M. Yalisove, Silicon surface morphologies after femtosecond laser irradiation, MRS Bull. 31 (2006) 626–633.
[29] Y. Peng, Y. Wen, D. Zhang, S. Luo, L. Chen, Y. Zhu, Optimal proportional relation between laser power and pulse number for the fabrication of surface-microstructured silicon, Appl. Optics 50 (2011) 4765–4768.
[30] C. Zhang, J. Yao, C. Li, Q. Dai, S. Lan, V.A. Trofimov, T.M. Lysak, Asymmetric femtosecond laser ablation of silicon surface governed by the evolution of surface nanostructures, Opt. Express 21 (2013) 4439–4446.
[31] Y. Peng, D. Zhang, H. Chen, Y. Wen, S. Luo, L. Chen, K. Chen, Y. Zhu, Differences in the evolution of surface-microstructured silicon fabricated by femtosecond laser pulses with different wavelength, Appl. Optics 51 (2012) 635–639.
[32] M. Huang, F. Zhao, Y. Cheng, N. Xu, Z. Xu, Origin of laser-induced near sub-wavelength ripples: interference between surface plasmons and incident laser, ACS Nano 3 (2009) 4062–4070.
[33] T. Tomita, Y. Fukumori, K. Kinoshita, S. Matsuo, S. Hashimoto, Observation of laser-induced surface waves on flat silicon surface, Appl. Phys. Lett. 92 (2008) 013104.
[34] J. Bonse, A. Rosenfeld, J. Kruger, On the role of surface plasmon polaritons in the formation of laser-induced periodic surface structures upon irradiation of silicon by femtosecond-laser pulses, J. Appl. Phys. 106 (2009) 104910.
[35] L. Hong Rusli, X.C. Wang, H.Y. Zheng, H. Wang, H.Y. Yu, Femtosecond laser fabrication of large-area periodic surface ripple structure on Si substrate, Appl. Surf. Sci. 297 (2014) 134–138.
[36] D. Mills, K.W. Kolasinski, Solidification driven extrusion of spikes during laser melting of silicon pillars, Nanotechnology 17 (2006) 2741–2744.
[37] K.W. Kolasinski, Solid structure formation during the liquid/solid phase transition, Curr. Opin. Solid St. M. 11 (2007) 76–85.
[38] B.K. Nayak, M.C. Gupta, K.W. Kolasinski, Spontaneous formation of nanospiked microstructures in germanium by femtosecond laser irradiation, Nanotechnology 18 (2007) 195302.
[39] J.E. Carey, C.H. Crouch, M. Shen, E. Mazur, Visible and near-infrared responsivity of femtosecond-laser microstructured silicon photodiodes, Opt. Lett. 30 (2005) 1773–1775.
[40] R.A. Myers, R. Farrell, A.M. Karger, J.E. Carey, E. Mazur, Enhancing near-infrared avalanche photodiode performance by femtosecond laser microstructuring, Appl. Opt. 45 (2006) 8825–8831.
[41] M.J. Smith, M. Winkler, M. Sher, Y. Lin, E. Mazur, S. Gradecak, The effects of a thin film dopant precursor on the structure and properties of femtosecond-laser irradiated silicon, Appl. Phys. A 105 (2011) 795–800.
[42] C. Wu, C.H. Crouch, L. Zhao, E. Mazur, Visible luminescence from silicon surfaces microstructured in air, Appl. Phys. Lett. 81 (2002) 1999–2001.
[43] T. Chen, J. Si, X. Hou, S. Kanehira, K. Miura, K. Hirao, Luminescence of black silicon fabricated by high-repetition rate femtosecond laser pulses, J. Appl. Phys. 110 (2011) 073106.
[44] Y. Ma, H. Shi, J. Si, T. Chen, F. Yan, F. Chen, X. Hou, Photoinduced microchannels and element change inside silicon by femtosecond laser pulses, Opt. Commun. 285 (2012) 140–142.
[45] Y. Ma, H. Ren, J. Si, X. Sun, H. Shi, T. Chen, F. Chen, X. Hou, An alternative approach for femtosecond laser induced black silicon in ambient air, Appl. Surf. Sci. 261 (2012) 722–726.